

Phase-shift interferometry measured transmission matrix of turbid medium: Three-step phase-shifting interference better than four-step one

Xi-Cheng Zhang(张熙程), Zuo-Gang Yang(杨佐刚), Long-Jie Fang(方龙杰), Jing-Lei Du(杜惊雷), Zhi-You Zhang(张志友), and Fu-Hua Gao(高福华)

Citation: Chin. Phys. B, 2021, 30 (**10**): 104202. DOI: 10.1088/1674-1056/abe92a
Journal homepage: http://cpb.iphy.ac.cn; http://iopscience.iop.org/cpb

What follows is a list of articles you may be interested in

Absorption interferometer of two-sided cavity

Miao-Di Guo(郭苗迪) and Hong-Mei Li(李红梅)
Chin. Phys. B, 2021, 30 (**5**): 054202. DOI: 10.1088/1674-1056/abdea4

Three-dimensional spatial multi-point uniform light focusing through scattering media based on feedback wavefront shaping

Fan Yang(杨帆), Yang Zhao(赵杨), Chengchao Xiang(向成超), Qi Feng(冯祺), and Yingchun Ding(丁迎春)
Chin. Phys. B, 2021, 30 (**4**): 044207. DOI: 10.1088/1674-1056/abe3e6

Far-zone behaviors of scattering-induced statistical properties of partially polarized spatially and spectrally partially coherent electromagnetic pulsed beam

Yan Li(李艳), Ming Gao(高明)†, Hong Lv(吕宏), Li-Guo Wang(王利国), and Shen-He Ren(任神河)
Chin. Phys. B, 2020, 29 (**10**): 104201. DOI: 10.1088/1674-1056/ab9de7

Memory effect evaluation based on transmission matrix calculation

Ming Li(李明), Long-Jie Fang(方龙杰), Lin Pang(庞霖)
Chin. Phys. B, 2019, 28 (**7**): 074207. DOI: 10.1088/1674-1056/28/7/074207

Rapid measurement of transmission matrix with the sequential semi-definite programming method

Zhenfeng Zhang(张振峰), Bin Zhang(张彬), Qi Feng(冯祺), Huimei He(何惠梅), Yingchun Ding(丁迎春)
Chin. Phys. B, 2018, 27 (**8**): 084201. DOI: 10.1088/1674-1056/27/8/084201

Phase-shift interferometry measured transmission matrix of turbid medium: Three-step phase-shifting interference better than four-step one

Xi-Cheng Zhang(张熙程), Zuo-Gang Yang(杨佐刚), Long-Jie Fang(方龙杰)†,
Jing-Lei Du(杜惊雷)‡, Zhi-You Zhang(张志友), and Fu-Hua Gao(高福华)

College of Physics, Sichuan University, Chengdu 610065, *China*

(Received 20 January 2021; revised manuscript received 15 February 2021; accepted manuscript online 24 February 2021)

Transmission matrix (TM) is an important tool for controlling light focusing, imaging, and communication through turbid media. It can be measured by 3-step (TM3) or 4-step (TM4) phase-shifting interference, but the similarities and differences of the transmission matrices obtained by the two methods are rarely reported. Therefore, we make a quantitative comparison of the peak light intensity, signal-to-noise ratio, and average background of $24 \times 24 = 576$ focal points between paired samples (TM3–TM4) through the Wilcoxon rank sum test, and discuss the singular value of the transmission matrix and the focal peak. The comparative results of peak light intensity and signal-to-noise ratio show that there is a significant difference between the 3-step phase shift and the 4-step phase shift transmission matrixes. The focusing effect of the former is significantly better than that of the latter; interest concentrates on the focal intensity and singular value. The reciprocal of the singular value is proportional to the squared intensity, which is in accordance with singular value theory. The results of comparison of peak light intensity and signal-to-noise ratio strongly suggest that 3-step phase shift should be selected and used in applying the phase shift method to the measurement of the transmission matrix; and the singular value is of great significance in quantifying the focusing, imaging, and communication quality of the transmission matrix.

Keywords: scattering media, phase modulation, transmission matrix, focal point

PACS: 42.25.Hz, 42.30.Rx, 78.20.–e **DOI:** 10.1088/1674-1056/abe92a

1. Introduction

Light scattering is a ubiquitous physical phenomenon in nature: in gases, liquids, and solids, and including turbid media such as clouds, milk, and white paint.[1–5] The phenomenon stems from the non-uniformity of refractive index[6] of the medium on a microscopic or mesoscopic scale, and touches a very wide range of research fields and applications, including among many others, atmospheric optics,[7] marine optics,[8] and biomedical photonics.[9] In recent years, research on light scattering has advanced dramatically. For example, the Anderson localization phenomenon[10] in the super-scattering process has been observed experimentally; the correlation of scattering with the microscopic geometric structures of turbid media has been discovered; and memory effects[11,12] have been studied, with applications to expanded fields of view,[13] speckle-related imaging,[14] and spectral memory effects,[15] and others. Especially important is the application of wavefront shaping technology to ultrasound,[16,17] optics, and interdisciplinary areas.[18] More recently, the focusing[9] and super-resolution imaging[9,18] of light in deep biological tissues were realized. It is expected that in the near future, wavefront shaping will become an important technical means for the integration of light scattering with other disciplines.

In the past decade, wavefront shaping has made great progress as a means of suppressing light scattering effects.[19] The rise of this technology is inseparable from spatial light modulators (SLM) that can control light on a micrometer scale.[20] Such a control can be achieved through wavefront shaping technologies[1] such as iterative feedback algorithm,[1,3] intelligent optimization algorithm,[21] neural network algorithm,[22] and transmission matrix (TM) method.[23,24] In 2010, Popoff *et al*. used an SLM combined with full-field phase-shifting interferometry to measure monochromatic light TM (a measure of transfer function)[23] in turbid media. Based on this pioneering work, many methods of measuring TM were discovered.[25–29] Yu *et al*. reported TM based on angular spectrum theory,[30] and Dremeau *et al*. used a digital micromirror device (DMD) to measure amplitude-type TM.[25] The most widely used method of measuring TM is full-field phase shift interferometry. The optical setup for this technique is simple and easy to operate, and is also robust and repeatable.

However, the scale of the turbid medium TM is huge,[31] and the 4-step phase shift method of measuring TM (hereinafter denoted by TM4 unless otherwise stated) has two major problems: (i) it needs to traverse a large number of input bases, which is time-consuming and requires to collect a large

†Corresponding author. E-mail: 1504450287@qq.com
‡Corresponding author. E-mail: dujl@scu.edu.cn

© 2021 Chinese Physical Society and IOP Publishing Ltd

number of data;[32] (ii) multiple phase shifts greatly increase the amount of data collection and memory overhead, and also increase the cost of collection time. In order to cope with these challenges, Conkey *et al*. found that TM can be retrieved with data for only three phase shifts (hereinafter denoted by TM3 unless otherwise stated).[33] The problem is whether there are appreciable differences between the TMs retrieved by the two methods. It is necessary to make sure which provides better optical transmission effect. The results of focusing experiments reported here show that TM3 is better than TM4 in both peak light intensity and signal-to-noise ratio. This result is consistent with the theoretical prediction of TM's singular value (a measure of focus energy). Therefore, when measuring TM by the phase shift method, we strongly recommend using a 3-step phase shift. The result shows that in the case of descending order and normalization, the squared reciprocal of the singular value of TM is not only proportional to the peak light intensity of the focus, but exhibits, to good approximation, a law of linear change. This law can make the singular value an important indicator to quantify the effects of TM focusing.[30,34–36] imaging, or communication.

2. Principle

2.1. Transmission matrix

A turbid medium is a linear medium, and the relation between its output and input light fields can be accurately described by a Green's function.[24] After multiple scattering of light in a turbid medium, a random speckle pattern is formed, which contains the information about the monochromatic light TM of the medium, and can be measured by full-field phase shift interference. In the process of measuring TM, if SLM and charge-coupled device (CCD) respectively correspond to N input and M output free modes, the relation between the output field and the input field of the medium can be expressed as

$$E_m^{\text{out}} = \sum_{n=1}^{N} t_{mn} E_n^{\text{in}}, \tag{1}$$

where E_n^{in} $(n = 1,\ldots,N)$ and E_m^{out} $(m = 1,\ldots,M)$ are the n-th input mode and m-th output channel, respectively; t_{mn} is a complex number that relates E_n^{in} to E_m^{out}, specifying the linear transmission characteristics of the turbid medium; t_{mn} forms a matrix that corresponds to the TM of the medium. Equation (1) can be expressed as

$$\boldsymbol{E}_{\text{out}} = \boldsymbol{T}\boldsymbol{E}_{\text{in}}, \tag{2}$$

where $\boldsymbol{E}_{\text{in}}$ and $\boldsymbol{E}_{\text{out}}$ are the complex vectors of the input field and output field, respectively, and $\boldsymbol{T}$ is the TM of the scattering medium.

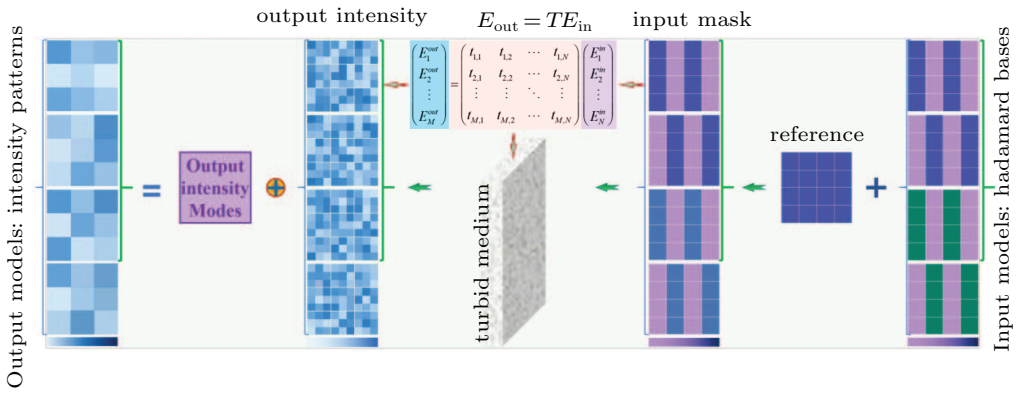


Fig. 1. Principle of TM measurement by phase shift method.

2.2. Principle of phase shift method

TM accurately characterizes the linear transmission characteristics of the turbid medium. In order to measure and access the TM, according to Eq. (2), we can find the TM by providing a specific input field $\boldsymbol{E}_{\text{in}}$ and measuring the corresponding output field $\boldsymbol{E}_{\text{out}}$. Because CCD can measure only light intensity, it is necessary to decouple TM from light intensity by providing an incident monochromatic plane wave for phase-shifting interferometry (Fig. 1),[23] where the interference light field is composed of static reference light R and signal light S. In order to perfectly match the SLM, we make a matrix with the Hadamard basis, which serves as the signal field S. In the process of phase shift interferometry (Fig. 1), the SLM needs to increase the relative phase shift φ (e.g. $\pi/2$)[37] three or four times in sequence. After each group of interference fields passes through the turbid medium, the CCD immediately collects the corresponding single group of feedback information. According to Eq. (1), the light intensity of the m-th output mode corresponding to the n-th input mode is

$$\begin{aligned} I_m^{\varphi} &= \left|E_m^{\text{out}}\right|^2 = \left|r_m + \textstyle\sum_n t_{mn} E\, \mathrm{e}^{\mathrm{i}\varphi}\right|^2 \\ &= |r_m|^2 + \left|\textstyle\sum_n t_{mn} E\, \mathrm{e}^{\mathrm{i}\varphi}\right|^2 + r_m^* \textstyle\sum_n t_{mn} E\, \mathrm{e}^{\mathrm{i}\varphi} \end{aligned}$$

$$+r_m\sum_n t_{mn}^* E^* \mathrm{e}^{-\mathrm{i}\varphi}, \tag{3}$$

where r_m represents the complex amplitude of the m-th reference light input mode. After using all Hadamard bases and collecting the corresponding feedback light intensity, the TM can be retrieved by using the feedback light intensity. In the process of measuring the TM, one can take $\varphi = 0$, $\pi/2$, π, and $3\pi/2$, and use the light intensity data ($\varphi = 0$, $\pi/2$, π, $3\pi/2$) collected by 3-step or 4-step phase shifts. From Eq. (3), one can construct a system of equations as follows:

$$I_m^0 = I_0 + r_m^*\sum_n t_{mn}E + r_m\sum_n t_{mn}^*E^*, \tag{4}$$

$$I_m^{\pi/2} = I_0 + \mathrm{i}r_m^*\sum_n t_{mn}E - \mathrm{i}r_m\sum_n t_{mn}^*E^*, \tag{5}$$

$$I_m^{\pi} = I_0 - r_m^*\sum_n t_{mn}E - r_m\sum_n t_{mn}^*E^*, \tag{6}$$

$$I_m^{3\pi/2} = I_0 - \mathrm{i}r_m^*\sum_n t_{mn}E + \mathrm{i}r_m\sum_n t_{mn}^*E^*, \tag{7}$$

where $I_0 = |r_m|^2 + \left|\sum_n t_{mn}E\,\mathrm{e}^{\mathrm{i}\varphi}\right|^2$. From Eqs. (4)–(6) or (4)–(7), the TM3 or TM4 can be derived as follows:

$$\sum_n t_{mn} = \frac{(\mathrm{i}+1)I_m^0 - 2\mathrm{i}I_{\mathrm{m}}^{\pi/2} + (\mathrm{i}-1)I_m^{\pi}}{4r^*E}, \tag{8}$$

$$\sum_n t_{mn} = \frac{(I_m^0 - I_m^{\pi}) - \mathrm{i}(I_m^{\pi/2} - I_m^{3\pi/2})}{4r_m^*E}. \tag{9}$$

After the TM is obtained, knowledge of it can be used to precisely control the energy transmission of light in a turbid medium, that is, focusing the light (Fig. 2).

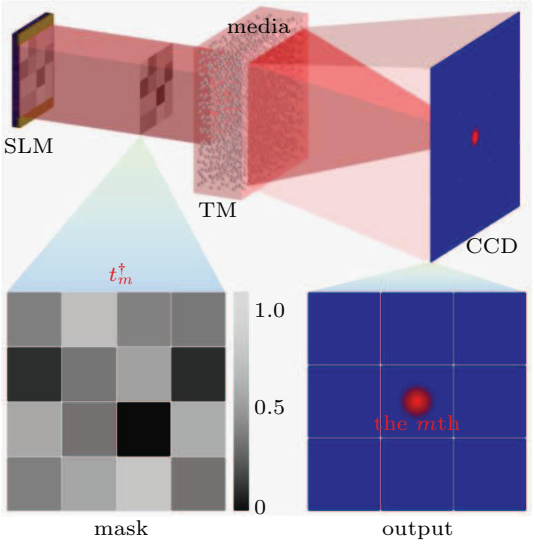


Fig. 2. Application of TM time inversion to focusing.

2.3. Relationship between singular value and focal energy

The light energy transmitted in the output mode can be measured by the singular value of the TM. In the process of time reversal and focusing, the target focus is usually set to be a unit output vector. For convenience and without loss of generality, we take the first focus as the target focus. Suppose $\boldsymbol{E}_1^{\mathrm{out}} \propto [1,0,\ldots,0]^{\mathrm{T}}$, then, according to Eq. (2), the input of the focus $\boldsymbol{E}_1^{\mathrm{in}}$ will be proportional to $\boldsymbol{E}_1^{\mathrm{out}}$, *i.e.*,

$$\boldsymbol{E}_1^{\mathrm{in}} \propto \boldsymbol{T}^{-1}\boldsymbol{E}_1^{\mathrm{out}}. \tag{10}$$

One can perform singular value decomposition (SVD) on $\boldsymbol{T}$ to obtain

$$\boldsymbol{T} = \boldsymbol{U}\boldsymbol{S}\boldsymbol{V}, \tag{11}$$

where $\boldsymbol{U}$ and $\boldsymbol{V}$ are both the unitary matrix, $\boldsymbol{S}$ is a diagonal matrix, and its diagonal elements are the singular values arranged from large to small. The reverse of Eq. (11) is

$$\boldsymbol{T}^{-1} = \boldsymbol{V}^{-1}\boldsymbol{S}^{-1}\boldsymbol{U}^{-1}. \tag{12}$$

From Eqs. (10) and (12), we obtain

$$\boldsymbol{E}_1^{\mathrm{in}} \propto \boldsymbol{V}^{-1}\boldsymbol{S}^{-1}\boldsymbol{U}^{-1}\boldsymbol{E}_1^{\mathrm{out}}. \tag{13}$$

When the time reversal technique is used to focus on the target (first) focus, the first line vector of $\boldsymbol{T}^{\dagger}$ († denotes the conjugate transpose) is used as the input phase $\boldsymbol{E}_1^{\mathrm{in}\dagger}$ of the focus, and the matrix product of $\boldsymbol{E}_1^{\mathrm{in}\dagger}$ and $\boldsymbol{T}$ is made. Since the row vectors of $\boldsymbol{T}$ are independent (orthogonal) under the multiple scattering mechanism, $\boldsymbol{T}\boldsymbol{E}_1^{\mathrm{in}\dagger}$ equals $\boldsymbol{E}_1^{\mathrm{in}}\boldsymbol{E}_1^{\mathrm{in}\dagger} = \left|\boldsymbol{E}_1^{\mathrm{in}}\right|^2 = I_1$. $\boldsymbol{V}$ and $\boldsymbol{U}$ are the unitary matrices and $\boldsymbol{E}_1^{\mathrm{out}}$ is the unit vector. Therefore, the CCD detects the light intensity at the target focus,

$$I_1 = \left|\boldsymbol{E}_1^{\mathrm{in}}\right|^2 \propto \left|\boldsymbol{V}^{-1}\boldsymbol{S}^{-1}\boldsymbol{U}^{-1}\boldsymbol{E}_1^{\mathrm{out}}\right|^2 = \left|\boldsymbol{S}_1^{-1}\right|^2. \tag{14}$$

Equation (14) shows that time reversal focusing is carried out through the transmission matrix, and the light intensity of the focus is proportional to the squared reciprocal of the singular value. Therefore, the larger the singular value of $\boldsymbol{T}$, the smaller the intensity value at the focal point is.

3. Experiment

The device for measuring the TM by the phase shift method and TM focusing is shown in Fig. 3. The laser passes through a microscope objective O_1 (40×, NA = 0.65) and a lens L_1 (focal length 100 mm). The beam splitter (BS) is used to reflect the continuous laser (λ = 632.8 nm) to the SLM (HOLOEYE PLUTO TELCO 1920 × 1080) and be coded (to the right directly through the unmodulated BS). The incident light is split into two beams. One of the beams which is not modulated by the SLM is background noise in this experiment and filtered by the pinhole "A", and the other is modulated by the SLM and passes through the pinhole. The physical principle of our optical setup is the same as the commonly used transmissive SLM. The pattern loaded in SLM is a series of orthogonal patterns, such as Hadamard patterns. The diaphragm is used to filter the background light which is not modulated by the SLM. The beam is then reduced by the 4f system L_2 (focal length 300 mm) and L_3 (focal length 100 mm), and focused on the front side of a (100 ± 20))-μm-thick turbid

medium comprised of polydimethylsiloxane (PDMS) and 5-μm-diameter alumina particles by the microscope objective lens O_2 (40×, NA = 0.65). After the light passing through the medium, the microscope objective O_3 (20×, NA = 0.40) collects light to illuminate the CCD (Canada Pointgrey, resolution 1920 × 1200@41 fps, pixel size 5.86 μm × 5.86 μm, working mode F7_Mono8_960 × 600_Mode1). The whole process of SLM and CCD is controlled by a computer (Dell: XPS 15-7590 1945T, Expanded Memory to 64 GB) in real time. In the 3-step phase-shifting interferometry, the phase shifts usually set to be 0, $2/3\pi$, and $4/3\pi$. The SLM needs to increase the relative phase shift φ (*e.g.* $2\pi/3$) three times in sequence. After each group of interference fields passes through the turbid medium, the CCD immediately collects the corresponding single group of feedback information. The intensity pattern in the output plane can be expressed as Eq. (3). In 4-step phase-shifting interferometry, the phase shifts are usually set to be 0, $1/2\pi$, π, $3/2\pi$. The SLM needs to increase the relative phase shift φ (*e.g.* $\pi/2$) four times in sequence. After each group of interference fields passes through the turbid medium, the CCD immediately collects the corresponding single group of feedback information. The intensity pattern in the output plane can be expressed as Eq. (3).

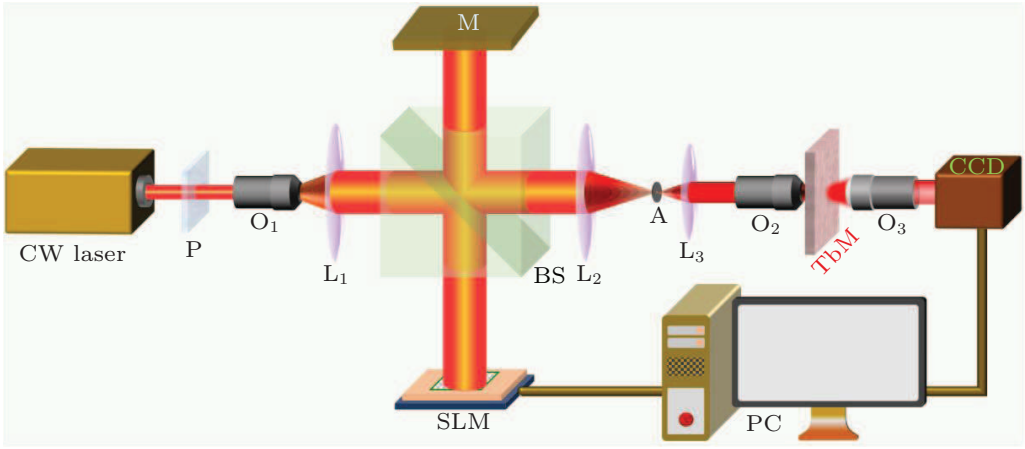


Fig. 3. Shematic diagram of device for measuring TM by phase shift method. CW laser: He–Ne laser. P: polarizer (transmission direction is aligned with SLM); SLM: spatial light modulator; CCD: charge-coupled device; PC: personal computer; L_1, L_2, L_3: lenses; O_1, O_2, O_3: microscope objective; BS: beam splitter; M: reflector; A: small aperture diaphragm; HM: turbid medium, a uniform mixture of cured PDMS (polydimethylsiloxane) and Al_2O_3 (alumina microspheres, with average diameter of about 5 μm).

4. Results

The propagation of light in the medium can be accurately controlled using the optical TM of a turbid medium. The TM can be measured by 3-step or 4-step phase-shift interference. In order to determine whether there is a significant difference between the TMs measured by these two methods, under the same instrument and parameter settings, we set 64×64 inputs (SLM controllable degrees of freedom) and 48×48 outputs (CCD controllable degrees of freedom). Comparison of the TM focusing effects on two outputs is performed. (i) The focusing effects of the first 4 focal points are compared qualitatively. (ii) The Wilcoxon rank sum test of paired samples (TM3–TM4) is used to quantitatively compare the peak light intensity with signal-to-noise ratio of $24 \times 24 = 576$ focal points in the field of view. (iii) The singular value (reciprocal) and energy transmission are then compared. Here we discuss the relation between singular value and light intensity. The paired comparison results of each focus are surprising: i) whether the peak light intensity and signal-to-noise ratio are compared qualitatively or quantitatively, TM3 is better than TM4, and ii) the singular value of TM3 is always smaller than that of TM4. What is even more interesting is that the squared reciprocal of the singular value is proportional to the light intensity. In addition, the application of TM3 focusing can not only obtain an excellent focusing effect, but also save 25% of the acquisition time, retrieval time, and memory overhead. Therefore, the focusing effect of TM3 is significantly better than that of TM4.

4.1. Qualitative contrast focusing effect

Intuitively, the effect of TM3 and TM4 focusing make us guess that there is a big difference between them. For comparison, in the case of 64×64 (input)–48×48 (output), we first qualitatively and intuitively compare the focal points of TM3 and TM4 at the same four positions (Fig. 4). The background intensity of the first and second focal point of TM3 (Figs. 4(a) and 4(b)) are slightly lower than those of TM4 (Figs. 4(c) and 4(d)), but the difference is not significant. However, the background intensity of the third and fourth focal point of TM3 (Figs. 4e and 4(f)) are significantly lower than those of TM4 (Figs. 4(g) and 4(h)). This comparison range is narrow (only 4 focal points). So, to be more general, we compare the 24×24 = 576 focal points in the field of view (see Supplementary Movie 3). The results show that the focusing effect of TM3 is significantly better than that of TM4.

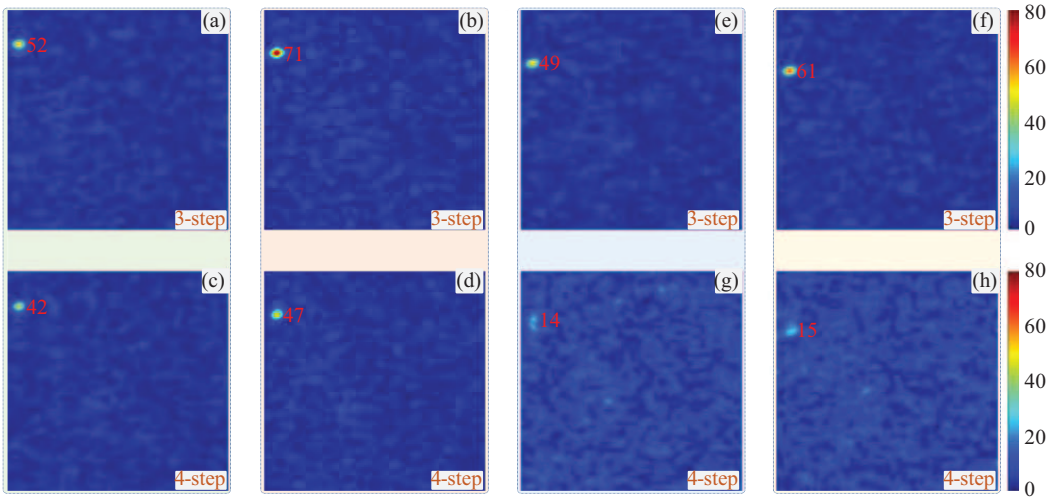


Fig. 4. Qualitative comparison among 4 focus effects before [(a), (c), (e), and (g)] 4-step phase shift and [(b), (d), (f), and (h)] 3-step phase shift for different target places, with red values being intensity values of focal points.

4.2. Quantitative comparison of peak light intensity and signal-to-noise ratio between TM3 focus and TM4 focus

The previous qualitative comparison is only a suggestive result. In order to quantitatively compare the focusing effect of TM3/4 in the case of 64×64–48×48, we take $24 \times 24 = 576$ focal points in the center of the field of view as the research target, and match the peak light intensity of each focal point with samples and signal noise. The Wilcoxon rank sum test is performed for the paired samples to compare their peak light intensities (quantified by the gray value of 0–255) and the differences in the signal-to-noise ratio (Fig. 5). The signal-to-noise ratio is defined as the ratio between the peak light intensity and the average background intensity. Among these 576 focal points, two cases are discussed below. The first case is that the median of the peak light intensity gray value using TM3 focusing is 76 (interquartile range 61–92); the median of the peak light intensity gray value using TM4 focusing is 36 (interquartile range 28–46) (Fig. 5(a)); the paired sample Wilcoxon rank sum test (Wilcoxon signed-rank test)[38] is performed on the two groups of light intensities, giving $P < 0.0001$, which is statistically significant (since $P < 0.025$), with P referring to the statistical difference between the two samples, and $P < 0.025$ means that there exists a large difference between the two samples. In statistics, the Mann–Whitney U test[38] (also called the Mann–Whitney–Wilcoxon (MWW),[39] Wilcoxon rank-sum test,[40] and Wilcoxon–Mann–Whitney test)[39] are all a nonparametric test.[38–40] This test can be used to determine whether two independent samples are selected from populations having the same distribution. The second case is that the median of the peak light intensity signal-to-noise ratio using TM3 focusing is 7.998 (interquartile range 6.561–9.605) (Fig. 5(b)); the median of the peak light intensity signal-to-noise ratio using TM4 focusing is 3.959 (interquartile range 3.097–4.985). The paired sample Wilcoxon rank sum test is performed on the peak light intensity signal-to-noise ratio of the two groups, giving $P < 0.0001$, which is also statistically significant (since $P < 0.025$).

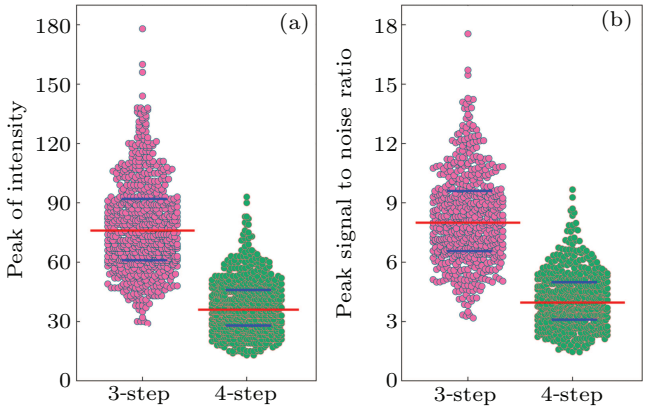


Fig. 5. (a) Peak light intensity and (b) signal-to-noise ratio of focal point using TM3 and TM4 in the 64×64–24×24 mode, where red circles represent 3-step, green circles denote 4-step, red line refers to average value of peak light intensity, and blue line means interquartile peak light intensity.

4.3. TM3 and TM4 focused average background contrast

The singular value, which is a measure of channel energy transmission, determines the total energy transmission efficiency and is a positive factor for TM focusing. Performing SVD on T^{-1} naturally includes the operation of reciprocating singular value. The smaller the singular value of T, the larger the corresponding reciprocal is and the greater the corresponding transmission energy, but with noise being amplified correspondingly. In the 64×64 mode, 551 (95.66%) of the 576 focal points focused by TM3 have a slightly higher background than TM4, and the average background gray value is less than 0.35 (Fig. 6(a)). In order to quantitatively compare the background noises of the two methods, we perform a Wilcoxon rank sum test on the paired samples of the average background. The median of the average background

light intensity gray value of TM3 focus is 9.490 (interquartile range 9.345–9.638) (Fig. 6(b)), while the median of the average background light intensity gray value of TM4 focus is 9.147 (interquartile range 9.043–9.250) (Fig. 6(b)). The paired sample Wilcoxon rank sum test is performed on the average background light intensity of the two groups, giving $P < 0.0001$, which is statistically significant (since $P < 0.025$).

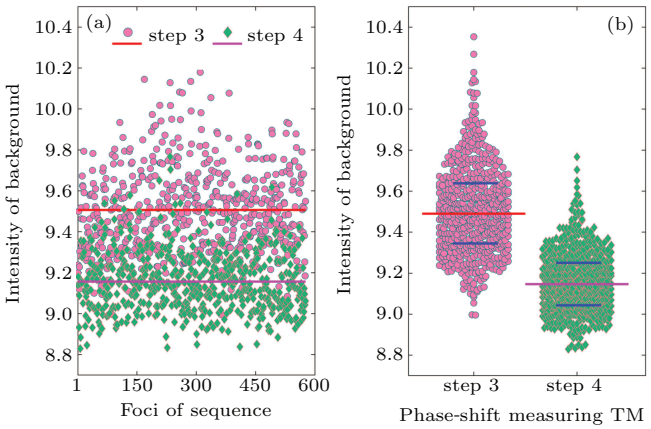


Fig. 6. (a) Intensity of background and (b) Wilcoxon rank sum test of background intensity and its statistical distribution for paired samples of average background, where red circles represent 3-step; green diamonds denote 4-step, red line refers to average light intensity obtained from method of 3-step average light intensity, magenta line means results obtained from method of 4-step average light intensity, and blue line is interquartile of peak light intensity.

4.4. Linear relationship between the singular value of the TM and the peak light intensity

4.4.1. Singular value of TM

The TM describes the transformation process of light passing through a turbid medium, and its singular value describes the characteristics of the transformation of light transmission by the medium, so the focusing effect is closely related to the singular value. Therefore, through SVD, a series of singular values of $24 \times 24 = 576$ output mode samples in the field of view (arranged from large to small) is obtained. The results show that the singular values of TM3/4 are in ranges of (687.11–22.04) and (992.06–26.40) (Figs. 7(a) and 7(b)). The most important thing is that TM3's singular value is smaller than TM4's for each pair of singular values. The difference between the singular values at the corresponding positions of the two is shown in Fig. 7(c) (the light green dashed line corresponds to zero difference). It is worth noting that due to the limitation of the numerical aperture of the microscope objective, the singular value distribution significantly devieates from the quarter-circle law predicted by the random matrix.[23,30]

4.4.2. Linear relationship between squared reciprocal of singular value and light intensity

Theoretically, the intensity of the focus is proportional to the squared reciprocal of singular value of the TM (see Section 3 and Fig. 8). In order to reduce the noise effect, we take 80% (10%–90%) of the 576 singular values to discuss its relation with the focus. The results are surprising: (I) the squared reciprocal of singular value of the TM fits the focus light intensity well [all arranged in descending order and normalized to the range 0 to 1, see Fig. 8(a)]; (II) squared reciprocals of the 80% singular value and the focal light intensity show a remarkable pattern of linear increase [see Fig. 8(b)].

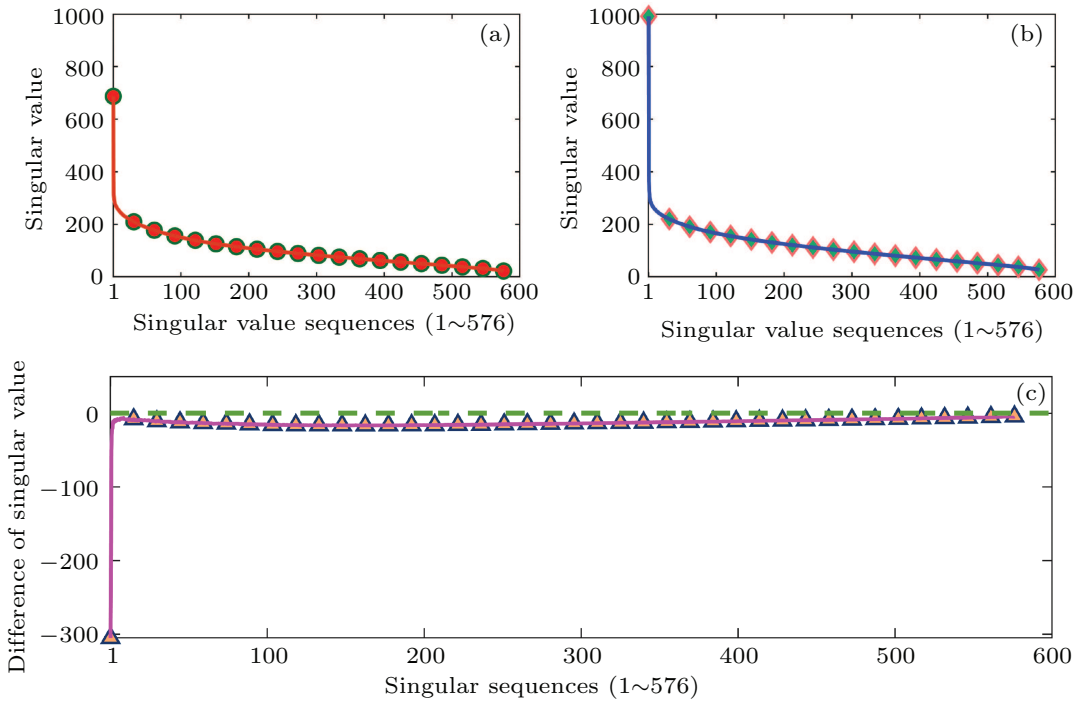


Fig. 7. Singular values of TM showing (a) singular value (σ_3) of TM3 and (b) singular value (σ_4) of TM4, and (c) singular value ($\Delta\sigma$) σ_3–σ_4.

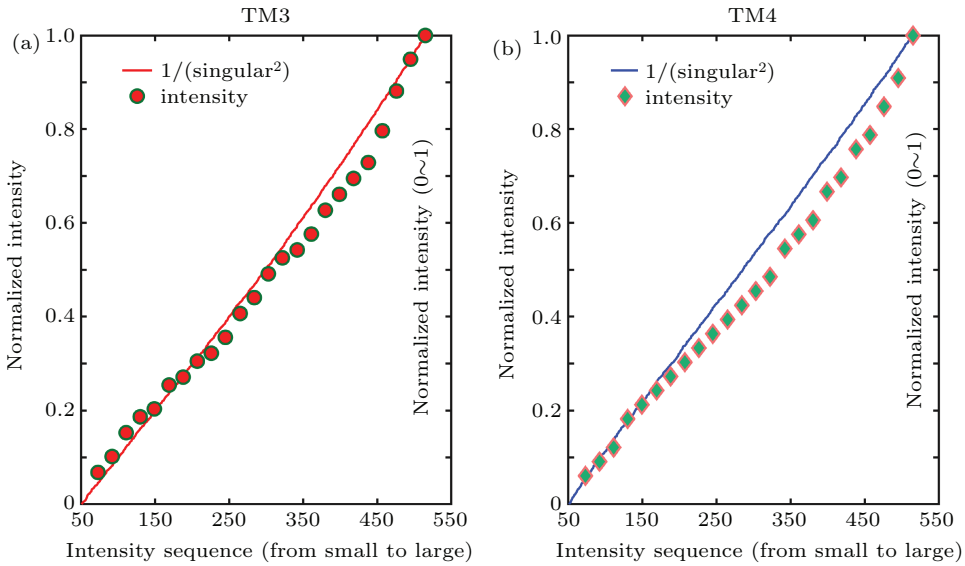


Fig. 8. Relations between singular value and intensity, showing (a) $(\sigma_3)^{-2}$ of middle 80% (10% to 90%) and corresponding peak light intensity, (b) $(\sigma_4)^{-2}$ of middle 80% (10% to 90%) and corresponding peak light intensity.

4.5. Acquisition time, memory, and retrieval time

When measuring the TM by the phase shift method, it is first necessary to traverse all input bases to obtain the data containing the TM information, and then to retrieve these data to obtain the subsequent TM. This implies that there are two problems: the process is time-consuming and it has high hardware overhead. In the 64×64 mode, TM3 has 25% less in acquisition and retrieval time than TM4, while also reducing memory overhead by 25% [see Figs. 9(a) and 9(b)].

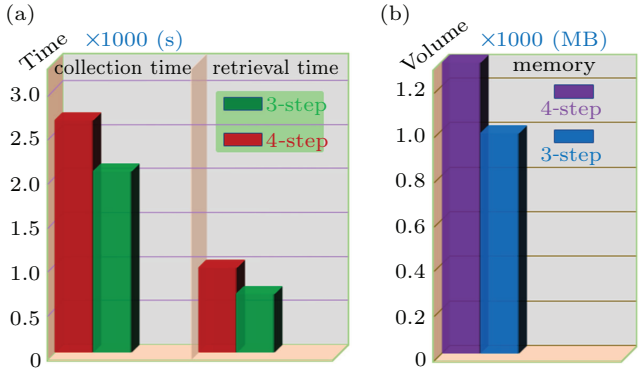


Fig. 9. (a) Acquisition time and retrieval time, (b) memory.

5. Discussion

Our results show that when the settings in the text are in 64×64 mode, there are significant differences between TM3 and TM4 as follows.

I) The peak light intensity and signal-to-noise ratio of TM3 focus are significantly better than those of TM4 (Figs. 4 and 5; Movie-2).

II) The paired singular values of TM3 and TM4 show a significant difference. The largest difference is huge, and TM3 is less than TM4 in all of the 576 singular values studied (Fig. 6(c)).

The results of time reversal and focusing show that the performance of TM3 in controlling light energy transmission is clearly more advantageous than that of TM4, which is in good agreement with the prediction by singular value theory: the squared reciprocal of the TM singular value is proportional to the focal light intensity (Figs. 7 and 8). The singular value of TM is a quantitative indicator of peak light intensity.[23,30,34] Based on the singular value results of TM3/4, it can be seen that TM3 is significantly better than TM4 in terms of controlling light transmission and suppressing noise. We believe that the reason is that the data collected by measuring TM3 has 25% less in noise (environmental noise, electronic noise, *etc.*) than by measuring TM4 (the former is collected three times, and the latter four times).

5.1. Illusion of background noise

Based on the theoretical prediction of singular values, the background noise of TM3 is theoretically higher than that of TM4. Figure 4 clearly indicates that the background of TM3 is lower than that of TM4. However, the results of quantitative background analysis prove the correctness of the theoretical prediction (Figs. 6 and 10). This statistical distribution is in good agreement with theoretical predictions. The reason for the illusion created by Fig. 4 is that the application software always adaptively maps the light intensity detected by the CCD into the range of gray values 0–255. Normally, the average peak light intensity of TM3 is higher than that of TM4, in fact by a factor of nearly 2.5. In the case that the mean values of the average backgrounds (TM3, 9.5066; TM4, 9.1568) are not much different from each other, the background of TM4 is magnified nearly 2.5 times on average, and the focus of TM4 will naturally show higher background noise. When we map

the TM3/4 focus into the background range (gray values 7–20), or the peak light intensity range, we see the real results as follows: the background of TM3 is slightly higher than that of TM4 as shown in green ellipse in Fig. 10, while the focal light intensity of TM3 is significantly higher than that of TM4 as shown by the red ellipse in Fig. 10. The gray value of the background intensity is in a range of gray values 29–178, and the gray value of the focal point is in a range of gray values 13–93. However, this illusion can be avoided by the contrast of peak light intensity to signal-to-noise ratio.

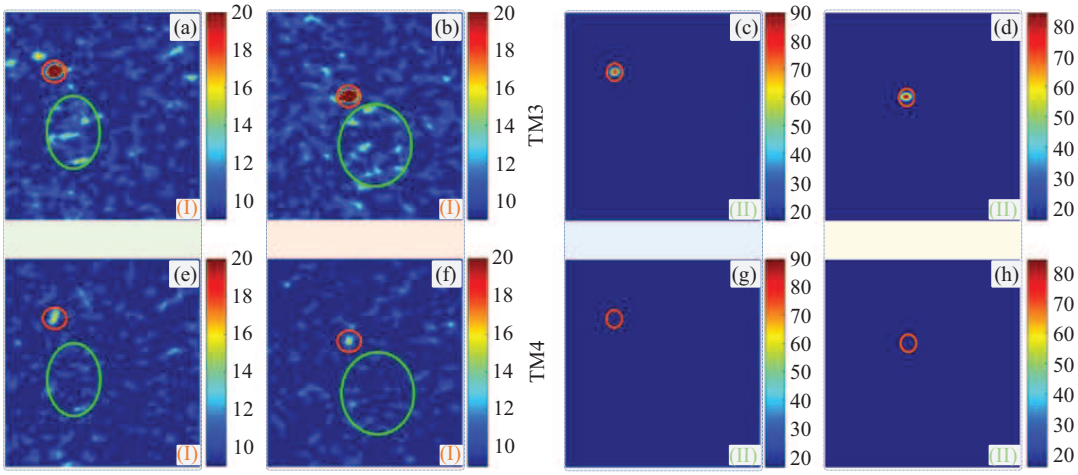


Fig. 10. Effect of normalizing focus intensity. (I) and (II) display background (7–20) and foci light intensity (20–80) respectively. The first and second row focus for TM3 and TM4 respectively. Panels (a)–(d) are for focus (1), and [(e)–(h)] for focus (II).

5.2. Deviation of singular values from quarter-circle law predicted by random matrix

In the process of measuring the TM by the phase shift method, the influence of noise is inevitable. In the process of data acquisition, the transmission of light in a turbid medium evolves in time (in the positive direction), and some very small singular values will be overwhelmed by noise effects. When light is focused by using the time reversal technology (corresponding to the matrix inversion $\boldsymbol{T}^{-1}$), some extremely large singular values (the squares of the extremely small reciprocals) will also be annihilated by noise. In order to reduce the noise effect, we take the middle 80% of the 576 focal points (arranged in descending order of light intensity) as the research object, and find that the reciprocal squares of the singular values maintain a good proportional relation with light intensity (Fig. 8), showing that the theoretical prediction and experimental results fit well. However, the linear change law of the singular value itself (Figs. 7(a), 7(b), 8(a), and 8(b)) seriously deviates from the quarter-circle law predicted by the random matrix.[23,30] We believe that the reason is the same as described in Ref. [30]. Owing to the limitation of the numerical aperture of the optical element, part of the light transmission mode is lost.

6. Conclusions

In summary, we report the substantial differences between the 3-step and 4-step phase shift measured TM3/4, differences that are common in 32×32, 64×64, and 128×128 input modes (Movie 1, Movie 2, and Movie 3). From all considered perspectives: theoretical prediction of singular values, experimental results of peak light intensity (total energy transmission efficiency), and signal-to-noise ratio (background noise suppression capability): TM3 behaves significantly better than TM4. Therefore, in the process of measuring TM by the phase shift method, we strongly recommend the 3-step method. While obtaining excellent transmission performance, the following additional benefits can be realized: data collection, memory cost, collection time and retrieval time can all be reduced by 25%. Most importantly, in the case of normalization, there is a consistent linear relationship between the squared reciprocal of the singular value and the peak light intensity. This important feature can be used to quantify the quality of TM focusing, imaging, and communication.

Supplementary materials: Movie 1–Movie 3

Supplementary materials Movie 1, Movie 2, Movie 3 for supporting content.

References

[1] Vellekoop I M and Mosk A P 2007 *Opt. Lett.* **32** 2309
[2] Vellekoop I M and Aegerter C M 2010 *Opt. Lett.* **35** 1245
[3] Vellekoop I M and Mosk A P 2008 *Opt. Commun.* **281** 3071
[4] Vellekoop I M and Mosk A P 2008 *Phys. Rev. Lett.* **101** 120601
[5] Vellekoop I M 2015 *Opt. Express* **23** 12189
[6] van Rossum M C W and Nieuwenhuizen T M 1999 *Rev. Mod. Phys.* **71** 313
[7] Wang Y 2008 *Journal of Aerosol Science* **39** 305
[8] Zhai P W, Hu Y X, Chowdhary J, Trepte C R, Lucker P L and Josset D B 2010 *J. Quantum Spectrosc. Radiat. Transfer.* **111** 1025
[9] Kim M, Choi W, Choi Y, Yoon C and Choi W 2015 *Opt. Express* **23** 12648

[10] Sperling T, Bührer W, Aegerter C M and Maret G 2013 *Nat. Photon.* **7** 48
[11] Judkewitz B, Horstmeyer R, Vellekoop I M, Papadopoulos I N and Yang C 2015 *Nat. Phys.* **11** 684
[12] Liu H, Liu Z, Chen M, Han S and Wang L V 2019 *Photon. Res.* **7** 1323
[13] He H, Guan Y and Zhou J 2013 *Opt. Express* **21** 12539
[14] Baek Y, Lee K, Oh J and Park Y 2020 *Sensors* **20** 3147
[15] Zhang H, Shao C, Kong W, Wang Y, Cao W, Liu C and Shen C 2017 *European Polymer Journal* **91** 376
[16] Chaigne T, Katz O, Boccara A C, Fink M, Bossy E and Gigan S 2013 *Nat. Photon.* **8** 58
[17] Horstmeyer R, Ruan H and Yang C 2015 *Nat. Photon.* **9** 563
[18] Beard P 2011 *Interface Focus* **1** 602
[19] Vellekoop I M, Cui M and Yang C 2012 *Appl. Phys. Lett.* **101** 081108
[20] Savage N 2009 *Nat. Photon.* **3** 170
[21] Conkey D B, Brown A N, Caravaca-Aguirre A M and Piestun R 2012 *Opt. Express* **20** 4840
[22] Haoyi Z, Zuogang Y, Longjie F and Shirong L 2018 *Laser Physics* **28** 096202
[23] Popoff S M, Lerosey G, Carminati R, Fink M, Boccara A C and Gigan S 2010 *Phys. Rev. Lett.* **104** 100601
[24] Popoff S M, Lerosey G, Fink M, Boccara A C and Gigan S 2011 *New J. Phys.* **13** 123021
[25] Dremeau A, Liutkus A, Martina D, Katz O, Schulke C, Krzakala F, Gigan S and Daudet L 2015 *Opt. Express* **23** 11898
[26] Yoon J, Lee K, Park J and Park Y 2015 *Opt. Express* **23** 10158
[27] Zhang H, Zhang B and Liu Q 2020 *Opt. Express* **28** 15006
[28] Boniface A, Gusachenko I, Dholakia K and Gigan S 2019 *Optica* **6** 274
[29] Tao X, Bodington D, Reinig M and Kubby J 2015 *Opt. Express* **23** 14168
[30] Yu H, Hillman T R, Choi W, Lee J O, Feld M S, Dasari R R and Park Y 2013 *Phys. Rev. Lett.* **111** 153902
[31] van Putten E and Mosk A 2010 *Physics* **3** 22
[32] Zhan L, Liu D, Yang A, Miao J and Zhu J 2019 *Appl. Opt.* **58** 2624
[33] Conkey D B, Caravaca-Aguirre A M and Piestun R 2012 *Opt. Express* **20** 1733
[34] Aubry A and Derode A 2009 *Phys. Rev. Lett.* **102** 084301
[35] Goetschy A and Stone A D 2013 *Phys. Rev. Lett.* **111** 063901
[36] Durand M, Popoff S M, Carminati R and Goetschy A 2019 *Phys. Rev. Lett.* **123** 243901
[37] Conkey D B, Caravaca-Aguirre A M and Piestun R 2012 *Opt. Express* **20** 1733
[38] Hollander M, Wolfe D A and Chicken E 2015 *Nonparametric Statistical Methods* (John Wiley & Sons) pp. 676–743
[39] Wilcoxon F 1945 *Individual Comparisons by Ranking Methods* (International Biometric Society, Wiley) pp. 80–83
[40] Gibbons J D and Chakraborti S 2011 *Nonparametric Statistical Inference* (Berlin, Heidelberg: Springer) pp. 20–32